Acoustic phonon behavior of PbWO$_4$ and BaWO$_4$ probed by low temperature Brillouin spectroscopy ☆

C. Kavitha [a,*], Chandrabhas Narayana [b], B.E. Ramachandran [a],
Nandini Garg [c], Surinder M. Sharma [c]

[a] Department of Chemistry—R&D Centre, BMSIT, Avalahalli, Yelahanka, Bangalore, Karnataka, India
[b] Jawaharlal Nehru Centre for Advanced Scientific Research (JNCASR), Jakkur P.O., Bangalore, Karnataka, India
[c] High Pressure & Synchrotron Radiation Physics Division, Bhabha atomic Research Centre, Mumbai, India

ARTICLE INFO

ABSTRACT

Temperature dependent acoustic phonon behavior of PbWO$_4$ and BaWO$_4$ using Brillouin spectroscopy has been explained for the first time. Low temperature Brillouin studies on PbWO$_4$ and BaWO$_4$ have been carried out from 320–20 K. In PbWO$_4$, we observe a change in acoustic phonon mode behavior around 180 K. But in the case of BaWO$_4$, we have observed two types of change in acoustic phonon mode behavior at 240 K and 130 K. The change in Brillouin shift ω and the slope dω/dT are the order parameter for all kinds of phase transitions. Since we do not see hysteresis on acoustic phonon mode behavior in the reverse temperature experiments, these second order phase transitions are not related to structural phase change and could be related to acoustic phonon coupled electronic transitions. In PbWO$_4$, the temperature driven phase transition at 180 K could be due to changes in the environment around the lead vacancy (V_{Pb}^{2-}) changes the electronic states. In the case of BaWO$_4$, the phase transition at 240 K shows the decrease in penetration depth of WO$_3$ impurity. So it becomes more metallic. The transition at 130 K could be the same electronic transitions as that of PbWO$_4$ as function of temperature. The sound velocity and elastic moduli of BaWO$_4$ shows that it could be the prominent material for acousto-optic device applications.

1. Introduction

Rare earth molybdate and tungstate materials have been actively studied by scientist because of their pronounced acousto-optic applications and cryogenic phonon scintillation detectors recently [1–3]. These materials can be doped with rare-earth ions. Such doped crystals have great importance in current study of optical maser [4]. Isostructural divalent metal molybdate and tungstate are important host materials for a variety of inorganic phosphors [5]. These materials are the host crystals for laser [6]. Structural phase transition, change in physical properties and spontaneous symmetry breaking of perovskites and rare-earth molybdates have been actively investigated by vibrational spectroscopy and neutron scattering spectroscopy [7–16]. Scheelite structured tungstate and molybdate are the main focus of recent spectroscopic studies at high temperature and high pressure, which exhibit several phase transitions [17]. However, it is still little known on their acoustic properties and its temperature behavior. It is relevant to study the similarities and differences among the structures belonging to the same type. It might help to determine the factors involved in structure stability. Further the influence of cation on the crystal structure can help in modeling the effect of impurities on the physical properties [18]. The introduction of cationic impurities in the host crystal can achieve the emission of laser light at desired frequencies [19]. The impurity strongly affects the emission properties of the crystal. Therefore the study of structural distortion in cation coordination can provide useful information for crystal growth and better understanding of the fine structure of the emission lines [20].

The most important factors affecting inter- and intra-atomic distances in solids and molecular solids are temperature, pressure and geometrical configurations. Temperature changes volume and excitations of the materials. Lowering the temperature could modify the environment of the system followed by electronic states. As a result change in elastic and optical properties will occur. To know about the nature of acoustic phonon coupled electronic states behavior, Brillouin spectroscopy could be used. The defects in cationic sites could have strong effect on the elastic properties and their temperature dependence signifies the phase

transition [21,22]. We have performed Brillouin studies on $PbWO_4$ and $BaWO_4$ as a function of low temperature ranging from 20 K to 320 K. i.e, one can cool the system from room temperature (320 K) to low temperature (20 K) and reverse experiments have been done by heating the system from 20 K to 320 K. We observe a phase transition at around 180 K for $PbWO_4$. But in the case of $BaWO_4$, we observe two phase transitions, one is at 240 K and the other is at 130 K. The reason for the phase transitions are discussed below.

2. Materials and experimental details

$PbWO_4$ crystal is grown in AT&T Bell laboratories, New Jersey as large single crystals by Czochralski technique [23]. $BaWO_4$ was made by the standard solid state route. Barium carbonate and tungsten oxide are mixed in their stoichiometric ratios and are finely ground together and then heated in a furnace. With the help of back-reflection Laue x-ray photograph, the plane of $PbWO_4$ and

$BaWO_4$ has been found as (001). Fig. 1a shows the representative Laue diffraction pattern of $BaWO_4$. The EDAX measurement of $PbWO_4$ shows the excess Pb in the form of PbO_2 impurity. But in the case of $BaWO_4$, we found the WO_3 impurity due to excess W in the system as shown in Fig. 1b. In $BaWO_4$, the Ba element concentration is 33.15% and the W element concentration is 66.85%. In $PbWO_4$ the element Pb concentration is 60.35% and the W element concentration is 39.65%.

Brillouin scattering measurements were carried out using 180° back scattering geometry with an incident angle of 45° with respect to surface normal. The schematic Brillouin spectroscopy experimental setup is shown in Fig. 2. The sample was mounted in a closed-cycle Helium Cryostat (CTI Cryogenic, USA). We used a temperature controller with silicon diode sensor (Conductus: Model LTC-10, USA). To determine the actual temperature of the sample, the thermal sensor was kept in contact with the sample on the copper sample holder. Temperature stability within ± 1 K was achieved during the measurement. Spectra have been recorded in lowering the temperature from 320 K to 20 K and
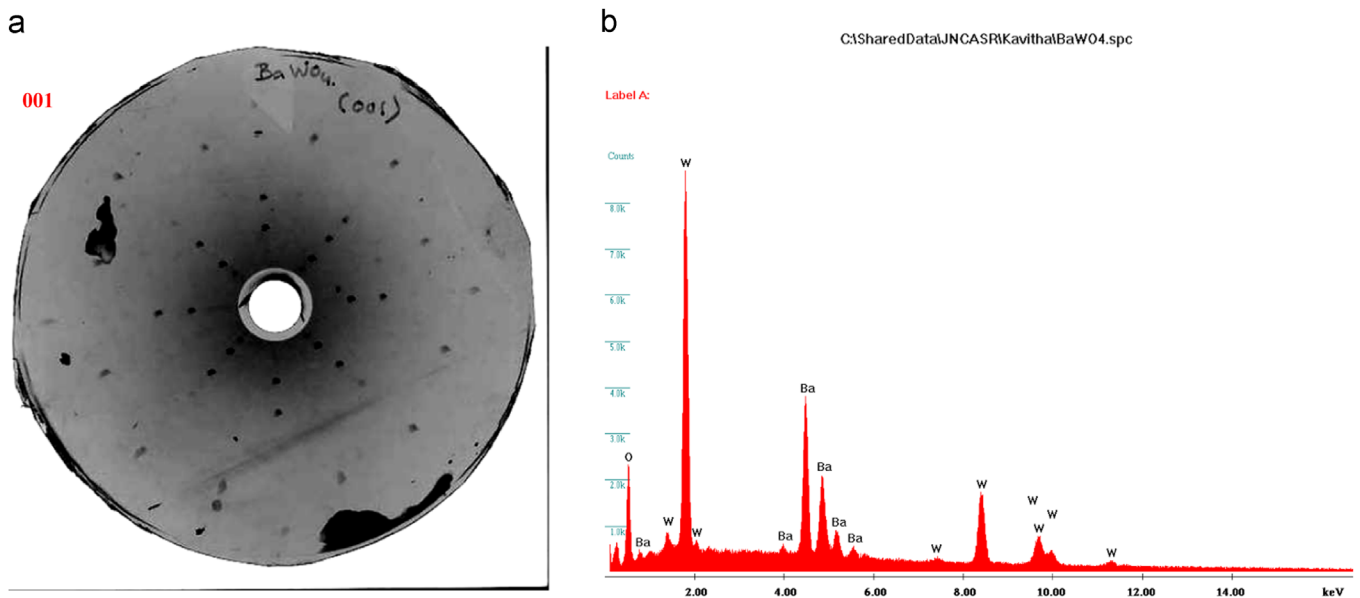

Fig. 1. (Color online) (a) Laue diffraction pattern of $BaWO_4$, and (b) EDAX spectrum of $BaWO_4$.
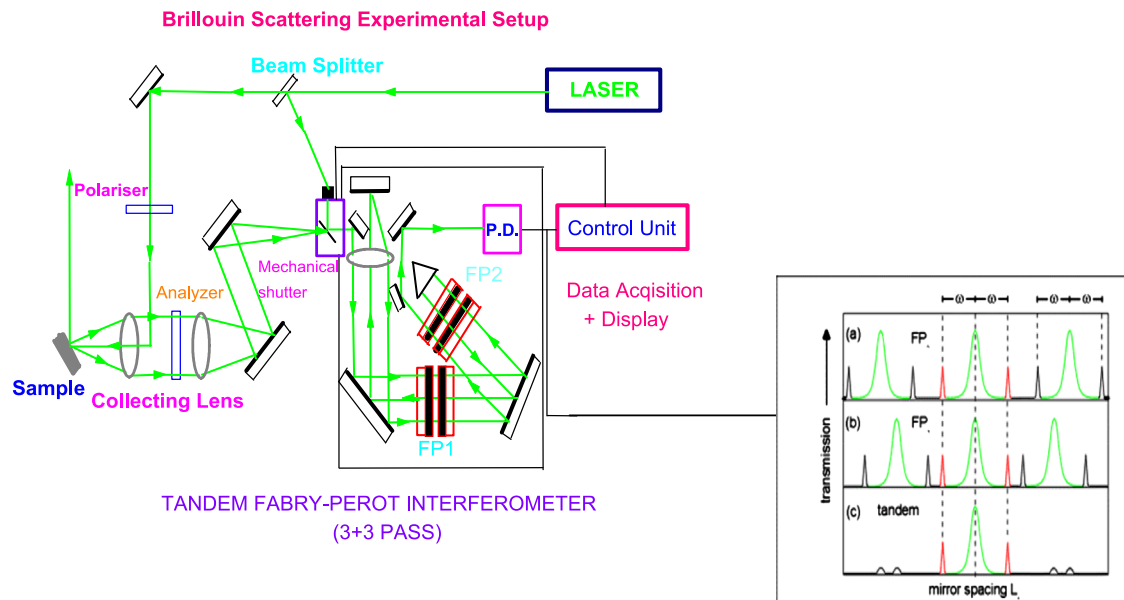

Fig. 2. (Color online) 180° Back scattering Brillouin experimental setup.

the reverse experiments have done with heating the sample from 20 K to 320 K. At each temperature, the spectra were recorded with a 30 min time interval. To perform Brillouin scattering, single mode vertically polarized Simple Harmonic Generation (SHG) of Nd-YAG laser operated at $\lambda = 532$ nm with 50 mW power is used as a light source. The collection optics was aligned in such a way that the spurious light scattering from the cryostat window was eliminated. The scattered light was polarized and analyzed by using JRS Scientific instruments $(3+3)$ pass tandem Fabry–Perot interferometer [24] equipped with a photo-avalanche diode detector which has finesse more than 100. Spectra reported in this work were recorded using a multi-channel scalar with 512 channels and the typical accumulations of 500–2000 passes were done with 0.768 s per pass. The line-shape parameters namely peak frequency, full width half maximum (FWHM) and area under the curve were extracted by a non-linear least square fitting of the data with a Lorentzian function, along with an appropriate background. The accuracy of FWHM obtained was an average of ± 0.5 GHz.

3. Theory of elastic constants

$PbWO_4$ and $BaWO_4$ crystallizes with the body centered tetragonal scheelite structure having space group $I4_1/a$. These compounds have four numbers of formula units per crystallographic cell at ambient condition [7]. The elastic properties depend on the orientation of the crystals. The elastic constant will give the internal properties of the crystal [25]. The velocity propagation 'v' of elastic waves in crystalline solid is given by the Cristoffel equation solution $(\Gamma_{jk} - \delta_{jk}\rho v^2)a_k = 0$, where $\Gamma_{jk} = \frac{1}{2}l_il_l(C_{ijkl} + C_{ijlk})$; $i,j,k,l = 1,2,3..$; δ_{jk} is the kronecker delta; and l_i is the direction cosines of the direction of propagation. The non-trivial solution for the above equation can be obtained, if the $|\Gamma_{ij} - \delta_{ij}\rho v^2| = 0$ secular equation is satisfied [26]. The roots of above equation will give the velocities of different waves propagated in a particular direction with in a solid. The plane of the crystal and the elastic wave propagation direction are the two prerequisites to calculate elastic constants.

Phonons can be labelled by the manner in which the vibrations occur. If the vibration occurs lengthwise in the direction of the wave and involves contraction and relaxation of the lattice, the phonon is called a longitudinal acoustic phonon (LA). Alternatively, the atoms

may vibrate side-to-side, perpendicular to the wave propagation direction; this is known as a transverse acoustic phonon (TA). In general, transverse vibrations tend to have smaller frequencies than longitudinal vibrations. The frequency measurement from Brillouin shift allows the determination of the velocity propagation in the elastic waves. The frequency shift of Brillouin line is given by $\Delta\nu/\nu = \pm (V_s/c) \ (n_i^2 + n_s^2 - 2n_in_s \cos \theta)^{1/2}$ where $\Delta\nu$ is the acoustic phonon frequency, ν is the frequency of incident light, V_s is the sound velocity of scattered phonon, c is the light velocity, n_i and n_s are the incident and scattered light refractive index, θ is the light scattering angle [27]. The sound velocity of the acoustic phonon is related to the elastic moduli C_{ij} through $V_s = \sqrt{(X/\rho)}$ where ρ is the density of crystal and X is the appropriate combination of elastic constants C_{ij} obtained by solving the equation of motion for a specific propagation direction. The calculation of elastic constants have been obtained for tetragonal crystal classes 4mm, 422, 42m, 4/mmm using above relation [28–30] and listed in Table 1 for certain direction of propagation.

4. Results

Fig. 3 shows, the polarization dependent Brillouin spectra of $PbWO_4$ and $BaWO_4$ at ambient conditions. The high frequency mode at 28 GHz is a longitudinal acoustic (LA) mode, the band at 11 GHz is the transverse acoustic (TA) mode and the 14 GHz is an acoustic phonon mode due to PbO_2 impurity for $PbWO_4$. Similarly, for $BaWO_4$, the high frequency mode at 26 GHz is LA mode, and the band at 10 GHz is TA mode of $BaWO_4$. Another sharp mode at 13 GHz is related to the WO_3 impurity for $BaWO_4$. The Brillouin spectra of $PbWO_4$ and $BaWO_4$ at different temperature are shown in Fig. 4. It is clear from the Fig. 4 that the impurity modes (namely 14 GHz and 13 GHz) for both $PbWO_4$ and $BaWO_4$ respectively are not affected by the temperature.

Table 1
Relation between elastic constants and sound velocity.

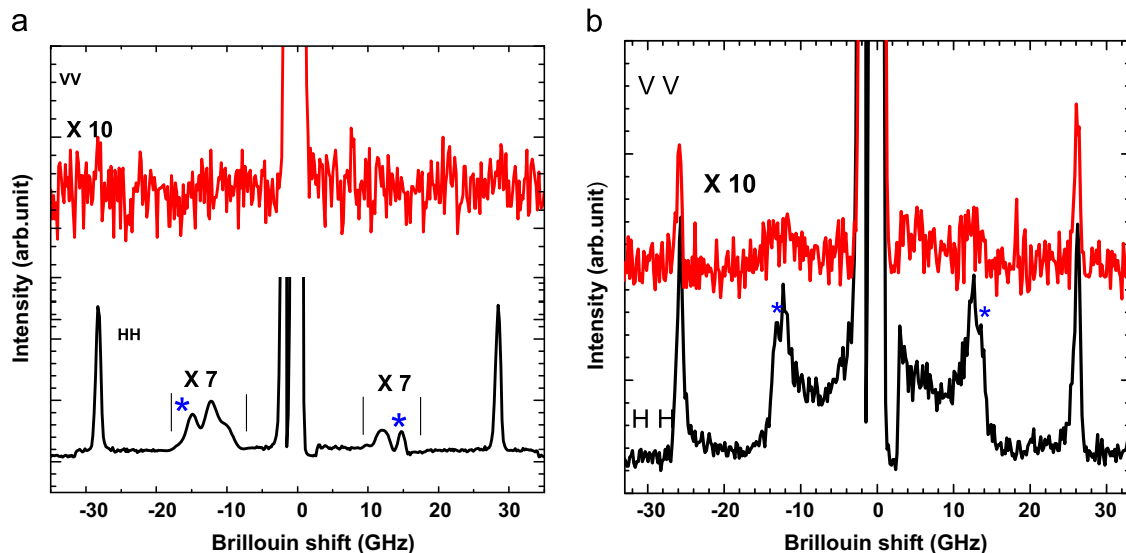| Direction cosines of propagation vector	Mode	Polarization direction	Velocity	Elastic constants
0,0,1	Pure longitudinal	[001]	v_1	$C_{33} = \rho v_1^2$
0,0,1	Pure shear	[100]	v_2	$C_{44} = \rho v_2^2$

Fig. 3. (Color online) Polarization dependent Brillouin Spectra of (a) $PbWO_4$ and (b) $BaWO_4$ at ambient conditions. The blue color star symbol indicates the modes due to impurity for both the compounds.

Table 2
The measurement of sound velocities and elastic moduli from pure LA and TA modes of $PbWO_4$.

Displacement direction	Propagation direction	Velocity, m/s, ultrasonic measurement, Ref [25]	Velocity, m/s (present work)	Elastic constants, $\times 10^{10}$ Nm^{-2}, ultrasonic measurement Ref [25]	Elastic constants, $\times 10^{10}$ Nm^{-2} (present work)
(0,0,1)	(0,0,1)	3355	3472 ± 50	$C_{33}=9.3$	$C_{33}=10.4 \pm 0.5$
(0,0,1)	(1,0,0)	1732	1770 ± 50	$C_{44}=2.5$	$C_{44}=2.7 \pm 0.5$

Table 3
The sound velocity and elastic constants of $BaWO_4$.

Displacement direction	Propagation direction	Velocity, m/s ($BaWO_4$) (present work)	Elastic constants for $BaWO_4$, $\times 10^{10}$ Nm^{-2} (present work)
(0,0,1)	(0,0,1)	3758	$C_{33}=9.1 \pm 0.5$
(0,0,1)	(1,0,0)	1879	$C_{44}=2.2 \pm 0.5$

Fig. 5 shows the temperature dependence of the TA mode frequency and corresponding full width half maximum (FWHM) for both the tungstate. The TA mode frequency increases with decrease in FWHM upon lowering the temperature. It is important to note that in the case of $BaWO_4$, we observe a change in slope at 240 K, but no change in FWHM. It is necessary to look at the LA data and would be discussed later.

Fig. 6 shows the temperature dependence of LA mode frequency and corresponding FWHM for both $PbWO_4$ and $BaWO_4$. In both the case, the Brillouin frequency increases with decrease in temperature. But the FWHM shows anomaly. At very low temperature FWHM of LA mode increases. This is anomalous and is observed in both the cases at 180 K for $PbWO_4$ and at 130 K for $BaWO_4$. In the case of $BaWO_4$, we find a discontinuity around 240 K in the mode frequency. It is interesting to note that we do not observe hysteresis around phase transitions for both the tungstate during reverse temperature experiment. This suggests that the transitions are second order in nature. The significance of this transition will be discussed later.

As discussed earlier, the room temperature elastic constants for both the compounds have been calculated (see Tables 2 and 3). We can elucidate two elastic constants C_{33}, C_{44} with following relations.

$$V_L = [C_{33}/\rho]^{1/2} \quad V_T = [C_{44}/\rho]^{1/2}$$

where V_L and V_T are the velocities calculated from longitudinal and transverse acoustic modes [28] and $\rho = m/V$ densitiy. The density of the $BaWO_4$ is 6349 kg/m^3 and the density of $PbWO_4$ is 8694 kg/m^3 [6-17]. This has good agreement with previous reports [25,31]. The respective velocities were calculated using the expression $[532 \times \Delta\upsilon]/[2n \times \sin(\theta/2)]$ where $\Delta\upsilon$ is the Brillouin shift, n the refractive index, θ is the scattering angle. The refractive index of $PbWO_4$ is 2.19 [32] and that of $BaWO_4$ is 1.84 [33].

5. Discussions

Theoretical calculations on the absorption spectra corresponding to the electronic transitions in $PbWO_4$ has made by LIU Ting et al. [34]. The calculated results indicate that the absorption band of the perfect $PbWO_4$ crystal does not occur in the visible region. However, the $PbWO_4$ crystal containing vacancy in the Pb site V_{Pb}^{2-} has two additional absorption bands in visible region. The two bands can be well decomposed into four Gaussian-shape bands observed at 350 nm, 405 nm, 550 nm and 670 nm which coincide well with the 350 nm, 420 nm, 550 nm and 680 nm absorption bands, respectively, measured in $PbWO_4$ crystals. Therefore, it can be concluded that the 350 nm, 420 nm, 550 nm and 680 nm

absorption bands are related to the existence of V_{Pb}^{2-} in the $PbWO_4$ crystal. Many reports have confirmed that it is difficult to get perfect crystal experimentally and the defect is more important for having absorption bands in the visible region. This is true in our case too. We observed PbO_2 impurities in $PbWO_4$ and WO_3 impurity in $BaWO_4$. The temperature dependent Raman studies on tungstate show no changes in the internal modes (WO_4) but they do see some softening of the external mode [35]. Unlike Raman vibrations acoustic phonons are long wavelength phonons and they are influenced by the network of atoms. Hence presence of impurity as well as the change of environment around the impurity would greatly modulate the acoustic phonons; hence we expect Brillouin spectra to be affected by the impurity.

In order to understand the differences in the behavior of $BaWO_4$ and $PbWO_4$, one can look at the polarized spectra of this tungstate as shown in Fig. 3. The polarization spectra of $PbWO_4$ in Fig. 3(a) shows the disappearance of all the modes with crossed polarization. This is expected. But in the case of $BaWO_4$, the LA mode persists in crossed polarization (see Fig. 3(b)). This suggests that there is a contribution from the excess WO_3 impurity to the LA mode. By lowering the temperature, one would find the difference in the LA mode behavior due to the bulk and impurity. This is the reason for the 240 K transition in $BaWO_4$. Correspondingly we observe an influence on TA mode as well. As one lowers the temperature, the volume contracts around the vacancy and large rearrangement will occur. The disappearance of TA mode signifies that the crystal tends towards an isotropic solid. This is also associated with a slight increase in the FWHM of LA mode in both the cases. It is important to note that the increase in FWHM means a change in life time of the phonon. As the vacancies are getting modulated, the electronic contribution is also getting modulated. Since LA mode is influenced by the vacancies, there is an increase in electron–phonon coupling leading to increase in FWHM and hence decrease in phonon life time.

Such a transition is not structural in nature which is corroborated by the fact that the transition is reversible without hysteresis. These results motivate one to look at the vacancies in cation sites and their use in the applications of the materials. According to Fig. 4(a,b), It is clear that the acoustic modes for $PbWO_4$ and $BaWO_4$ changes with lowering temperature. But the modes due to impurities for both the compounds do not see any changes with temperature. This has been marked with blue color star symbol in the spectra. The increase in TA mode as well as the decrease in FWHM with low temperature (see Fig. 5(a–d)) shows stiffening of the bonds as well as the reduction of average spread in spring constant for both the compounds. These modes seize to exist below 180 K and 130 K for $PbWO_4$ and $BaWO_4$ respectively. This could be due to contraction of WO_4 bonds with low temperature for both compounds. TA mode is influenced by the vacancies in both the compounds. In our case, TA mode seizes to exist beyond 180 °C and 130 °C for both the compounds. In order to know about the change in phonon coupled electronic states below these temperatures, one can analyze LA mode which is also strongly coupled to the electronic states [36]. According to LA mode behavior of $PbWO_4$ with temperature (see Fig. 6a), the mode frequency hardens with low temperature. But around 180 K, there is a change in slope observed. The behavior of FWHM with temperature in Fig. 6b shows increase in line width below 180 K. This is an anomalous behavior. This could be
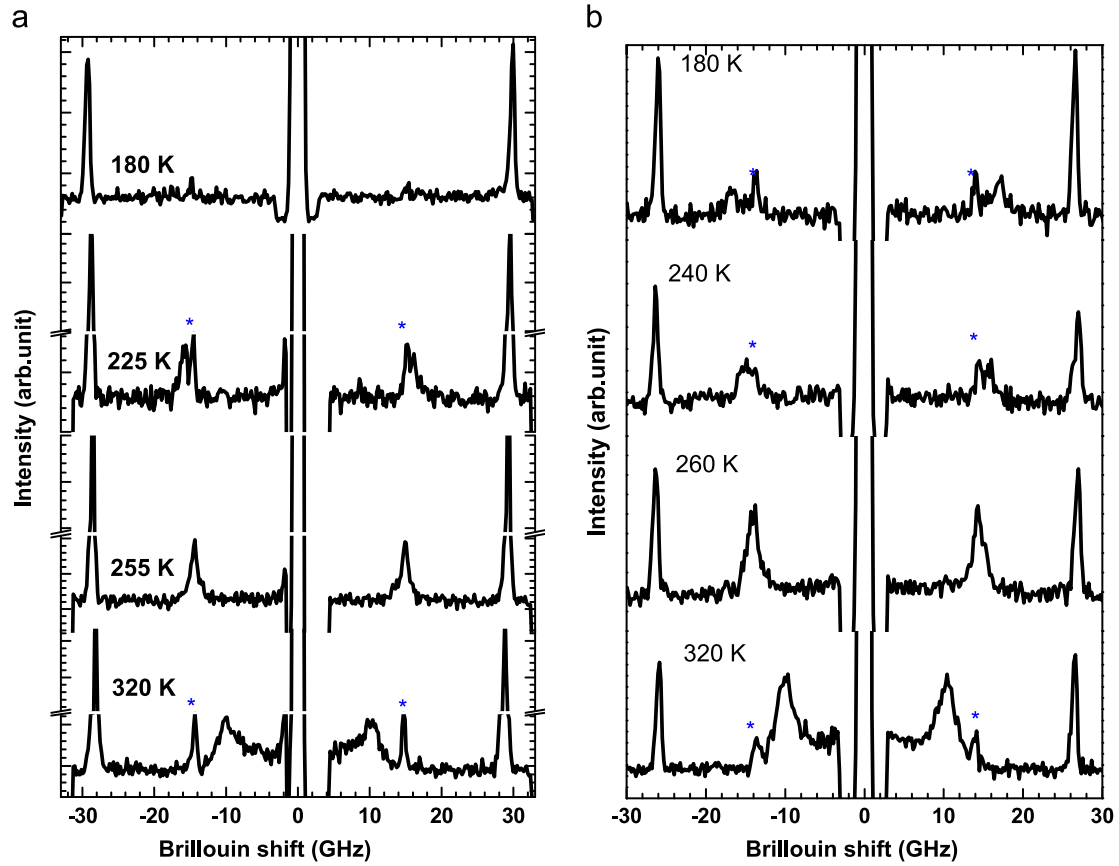
Fig. 4. (Color online) Low temperature Brillouin spectra of (a) PbWO$_4$ and (b) BaWO$_4$. The blue color star symbol indicates the modes due to impurity for both the compounds.
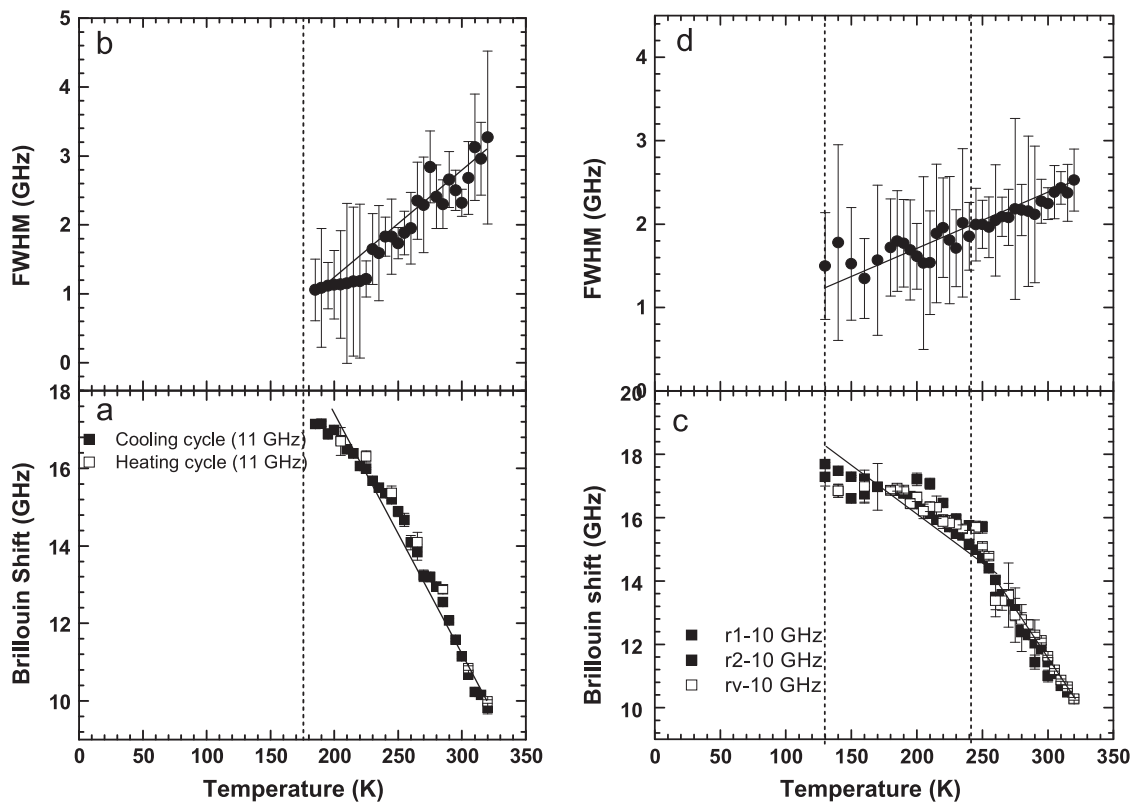

Fig. 5. (Color online) Temperature dependence of the (a) TA mode frequency, (b) FWHM for PbWO$_4$, and (c) TA mode frequency, (d) FWHM for BaWO$_4$. Solid symbol represents cooling cycle and open symbol represents heating cycle. Solid line shows linear fit to the data. Vertical dotted line shows the phase transitions.
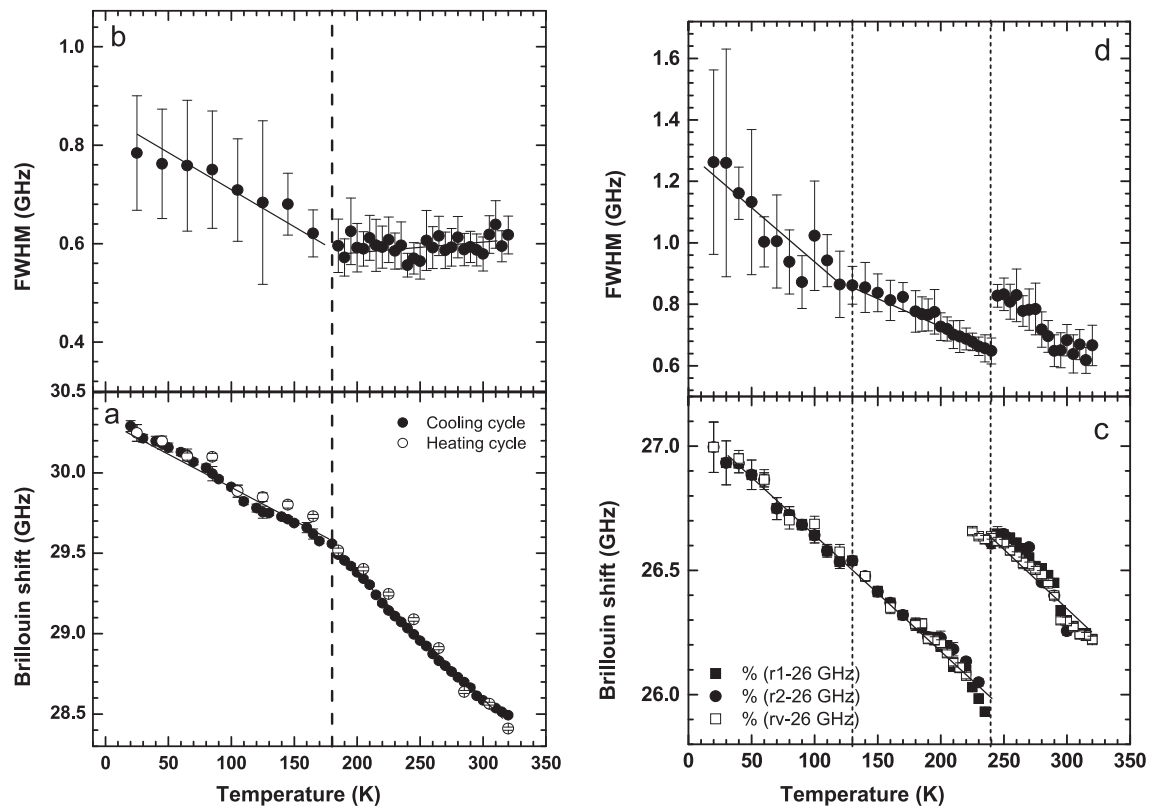
Fig. 6. Temperature dependence (a) LA mode frequency, (b) FWHM for $PbWO_4$, and (c) LA mode frequency, (d) FWHM for $BaWO_4$. Solid symbol represents cooling cycle and open symbol represents heating cycle. Solid line shows linear fit to the data. Vertical dotted line shows the phase transitions.

related to changes in environment due to contraction of the system with low temperature. This involves changes in electronic states. Since acoustic modes involve whole lattice vibration, there is a strong coupling between electronic states and phonon states. This reflects the change in phonon life time below 180 K. In the case of $BaWO_4$, we observe the hardening of frequency as well as increase in FWHM with lowering temperature (see Fig. 6(c,d)). This could be related to decrease in penetration depth as a result conductivity increases. So the WO_3 impurity becomes more metallic. The sudden discontinuity at 240 K could be related to disappearance of WO_3 impurity in the system. This phase transition is insensitive for x-ray because it can effectively probe structural phase change in the system. But brilouin spectroscopy has high resolution as compared to x-ray and can effectively probe change in physical property of the system without structural change. The change in slope in FWHM at 130 K could be related to changes in environment due to contraction of the system. This is related to changes in electronic states in the system. Due to strong electron–phonon coupling, these changes reflect in acoustic phonon modes with low temperature. As a result, there is an anomalous behavior in FWHM with low temperature. This electronic phase transition could be same as that of $PbWO_4$. The reversibility of these modes clearly shows that this phase transition is second order transition. This shows that there is no structural change for both the compounds.

6. Conclusion

In conclusion, we observe temperature induced phase transition for $PbWO_4$ and $BaWO_4$ using Brillouin scattering. The phase transition in this tungstate could be related to contraction of the system with low temperature which changes the environment around the cation vacancy Pb in the case of $PbWO_4$ and W in the case of $BaWO_4$. The vacancy cannot be avoided in these crystals

and are responsible for the presence of absorption in the visible range. The acoustic modes are linked with these electronic levels and hence show a strong electron–phonon interaction [36] upon modulation of these impurities with temperature. There is a decrease in life time of phonon due to this. The transition is second order in nature and is observed at 130 K for $BaWO_4$ and 180 K for $PbWO_4$. The 240 K transition in $BaWO_4$ is due to WO_3 precipitation and their contribution is minimal to the Brillouin spectra. So it is necessary to study these systems in the presence of these impurities. It would be interesting to carry out temperature dependent absorption studies of these materials to see the effect of strong electron–phonon interaction.

References

[1] Q. Xiandong, Compact Muon Solenoid (CMS), Technical Proposal, CERN/LHC 93, 1994, p. 1.
[2] M. Kobayashi, M. Ishi, Y. Usuki, H. Yahagi, Nucl. Instrum. Methods Phys. Res. A 333 (1993) 429.
[3] D. Errandonea, J. Pellicer-Porres, F.J. Manjan, A. Segura, C.h. Ferrer-Roca, R.S. Kumar, O. Tschauner, P. Rodriguez-Hernandez, J. Lopez-Solano, S. Radescu, A. Mujica, A. Munoz, G. Aquilanti, Phys. Rev. B 72 (2005) 174106.
[4] S.P.S. Porto, J.F. Scott, Phys. Rev. 157 (1967)716 157 (1967).
[5] Nicol Malcolm, Jean F. Durana, J. Chem. Phys. 54 (1971) 1436.
[6] W.W. Ge, H.J. Zhang, J.Y. Wang, J.H. Liu, X.G. Xu, X.B. Hu, M.H. Jiang, D.G. Ran, S.Q. Sun, H.R. Xia, R.I. Boughton, J. Appl. Phys. 98 (2005) 013542.
[7] G. Erdogan, D. Eugene, J.S. King, J. Chem. Phys. 55 (1971) 1093.
[8] Zalkin Allan, David H.Templeton, J. Chem. Phys. 40 (1964) 501.
[9] S. Etsuro, A. Yukikuni, K. Masakazu, J. Phy. Soc. Jpn. 54 (1985) 480.
[10] Y. Hirotaka, Y. Atsuo, U. Hiromoto, S. Tunetaro, Phys. Rev. B 43 (1991) 4473.
[11] R.O. Bell, G. Rupprecht, Phys. Rev. 129 (1963) 90.

[12] H. Yamaguchi, H. Uwe, T. Sakudo, E. Sawaguchi, J. Phy. Soc. Jpn. 57 (1988) 147.
[13] S. Akikatsu, U. Masayuki, N. Terutaro, Phys. Rev. Lett. 39 (1977) 829.
[14] E.T. Keve, S.C. Abrahams, J.L. Bernstein, J. Chem. Phys. 54 (1971) 3185.
[15] B.N. Ganguly, F.G. Ullman, R.D. Kirby, J.R. Hardy, Solid State Commun. 17 (1975) 533.
[16] V. Dvořák, Phys.Status Solidi B 46 (1971) 763.
[17] R.M. Hazen, L.W. Finger, J.W.E. Mariathasan, J. Phys. Chem. Solids 46 (1985) 253.
[18] L.E. Depero, L. Sangaletti, J. Solid State Chem. 129 (1997) 82.
[19] L. Zundu, H. Yindong, J. Phys. Condens. Matter. 6 (1994) 3737.
[20] L.E. Depero, L. Sangaletti, J. Solid State Chem. 119 (1995) 428.
[21] M. Mączka, F. Jiang, S. Kojima, J. Hanuza, J. Mol. Struct. 365 (2001) 563.
[22] D. Kasprowicz, T. Runka, M. Szybowicz, M. Drozdowski, A. Majchrowski, E. Michalski, J. Zmija, J. Mol. Struct. 139 (2006) 792.
[23] A. Jayaraman, B. Batlogg, L.G. VanUitert, Phys. Rev. B 31 (1985) 5423.
[24] S.M. Lindsay, M.W. Anderson, J.R. Sandercock, Rev. Sci. Instrum. 52 (1981) 1478.
[25] A.G. Khatkevich, Sov. Phys. Crystallogr. 6 (1962) 561.
[26] M. Gluyas, F.D. Hughes, B.W. James, J. Phys. D: Appl. Phys. 6 (1973) 2025.
[27] M.H. Grimditch, G.D. Holah, Phys. Rev. B 12 (1975) 4377.
[28] N.P. Kobelev, Soífer, Phys. Solid State 38 (1996) 1956.
[29] J.M. Farley, G.A. Saunders, J. Phys. C: Solid State Phys. 5 (1972) 3021.
[30] B.A. Auld, Acoustic Fields and Waves in Solids, vol. 1, 1973.
[31] G.A. Coquin, D.A. Pinnow, A.W. Warner, 42 (1971) 2162.
[32] D.R. Lide (Ed.), CRC Handbook of Chemistry and Physics, CRC, 1990.
[33] T.T. Basiev, A.V. Gavrilov, V.V. Osiko, S.N. Smetanin, A.V. Fedin, Quantum Electron. 34 (2004) 649.
[34] Y. Liu Ting, R. Zhang, L. Qi, Zhuang Song, Chin. Phys. Lett. 22 (2005) 442.
[35] J. Suda, T. Sato, J. Phys. Soc. Jpn. 66 (1997) 1707.
[36] C. Kavitha, N. Chandrabhas, Solid State Commun. 195 (2014) 10.